processes

MDPI

Article

# Green Synthesis of a Novel Silver Nanoparticle Conjugated with *Thelypteris glandulosolanosa* (Raqui-Raqui): Preliminary Characterization and Anticancer Activity

**Lucero Del Carmen Vera-Nuñez [1], Junior Oliver Cornejo-Ruiz [1], Carlos Alberto Arenas-Chávez [2], Luciana Maria de Hollanda [3], Aldo Alvarez-Risco [4], Shyla Del-Aguila-Arcentales [5], Neal M. Davies [6], Jaime A. Yáñez [7,8,*] and Corina Vera-Gonzales [1,9]**

1 Faculty of Natural Sciences, Department of Chemistry, National University of San Agustin de Arequipa, Arequipa 04000, Peru; lveran@unsa.edu.pe (L.D.C.V.-N.); jtamoc@unsa.edu.pe (J.O.C.-R.); cverag@unsa.edu.pe (C.V.-G.)
2 Laboratory of Biology and Cell Culture, Department of Biology, National University of San Agustin de Arequipa, Arequipa 04000, Peru; carenasc@unsa.edu.pe
3 Centro Universitário Metrocamp, Wyden University, Campinas-São Paulo 13035-350, Brazil; luciana.hollanda@professores.unimetrocamp.edu.br
4 Carrera de Negocios Internacionales Facultad de Ciencias Empresariales y Económicas, Universidad de Lima, Lima 15023, Peru; aralvare@ulima.edu.pe
5 Escuela Nacional de Marina Mercante "Almirante Miguel Grau", Callao 07021, Peru; sdelaguila@enamm.edu.pe
6 Faculty of Pharmacy & Pharmaceutical Sciences, University of Alberta, Edmonton, AB T6G 2H1, Canada; ndavies@ualberta.ca
7 Vicerrectorado de Investigación, Universidad Norbert Wiener, Lima 15046, Peru
8 Gerencia Corporativa de Asuntos Científicos y Regulatorios, Teoma Global, Lima 15073, Peru
9 Laboratory of Preparation, Characterization, and Identification of Nanomaterials (LAPCI_NANO), National University of San Agustin of Arequipa, Arequipa 04000, Peru
* Correspondence: jaime.yanez@uwiener.edu.pe

check for updates

**Citation:** Vera-Nuñez, L.D.C.; Cornejo-Ruiz, J.O.; Arenas-Chávez, C.A.; de Hollanda, L.M.; Alvarez-Risco, A.; Del-Aguila-Arcentales, S.; Davies, N.M.; Yáñez, J.A.; Vera-Gonzales, C. Green Synthesis of a Novel Silver Nanoparticle Conjugated with *Thelypteris glandulosolanosa* (Raqui-Raqui): Preliminary Characterization and Anticancer Activity. *Processes* **2022**, *10*, 1308. https://doi.org/10.3390/pr10071308

Academic Editor: Vilma Petrikaite

Received: 30 May 2022
Accepted: 21 June 2022
Published: 3 July 2022



**Abstract:** In the last decade, the green synthesis of nanoparticles has had a prominent role in scientific research for industrial and biomedical applications. In this current study, silver nitrate ($AgNO_3$) was reduced and stabilized with an aqueous extract of *Thelypteris glandulosolanosa* (Raqui-raqui), forming silver nanoparticles (*AgNPs-RR*). UV-vis spectrophotometry, dynamic light scattering (DLS), and scanning transmission electron microscopy (STEM) were utilized to analyze the structures of *AgNPs-RR*. The results from this analysis showed a characteristic peak at 420 nm and a mean hydrodynamic size equal to 39.16 nm, while the STEM revealed a size distribution of 6.64–51.00 nm with an average diameter of 31.45 nm. Cellular cytotoxicity assays using MCF-7 (ATCC® HTB-22™, mammary gland breast), A549 (ATCC® CCL-185, lung epithelial carcinoma), and L929 (ATCC® CCL-1, subcutaneous connective tissue of *Mus musculus*) demonstrated over 42.70% of MCF-7, 59.24% of A549, and 8.80% of L929 cells had cell death after 48 h showing that this nanoparticle is more selective to disrupt neoplastic than non-cancerous cells and may be further developed into an effective strategy for breast and lung cancer treatment. These results demonstrate that the nanoparticle surfaces developed are complex, have lower contact angles, and have excellent scratch and wear resistance.

**Keywords:** *Thelypteris glandulosolanosa*; green synthesis; AgNPs; breast cancer; lung cancer; Raqui-Raqui

## 1. Introduction

Breast and lung cancers are amongst the most frequently diagnosed cancers worldwide, causing over one million deaths annually [1–6]. Conventional cancer treatment shows several limitations, including low or no specificity and low efficacy in discriminating between neoplastic and healthy cells [7]. The typical treatments most commonly prescribed for these types of cancer include chemotherapy [8–10], which is administered

to therapeutically control tumor growth and prolong patient survival [11]. However, chemotherapy of anticancer drugs often have several limitations including vascular administration and extravasation, low or no oral bioavailability [12,13], rapid elimination [14], adverse side effects [15–17], non-specific off target cytotoxicity [13,17–20], and multidrug resistance [21,22].

For approximately 50 years, natural products have provided sources of chemotherapeutic molecules in combating cancer [16,23–33]. The primary sources of these successful compounds are plants from terrestrial environments [34,35]. Among several terrestrial plants, the ferns are widely distributed in the world, mainly in India [36,37], Türkiye [38], Nepal [39], Japan [40], and Peru [41–44], with some species having been used in food or folk medicine for centuries [45]. Ferns comprise over 12,000 species spread among 250 different genera [46]. The secondary metabolites of these ferns have been reported to have antioxidant [47,48], anti-inflammatory [49,50], anticancer [49,51,52], and antimicrobial [53] activities. Among these ferns, *Thelypteris torresiana* contains the secondary metabolites protoapigenin [54], flavotorresin [55,56], 2′-hydroxy-2′,3′-dihydroprotoapigenone acetonide [53], 2′,6′-dimethoxy-tetrahydroprotoapigenone [54], and tetrahydroprotoapigenone [55] that have antitumoral activity. *Thelypteris torresiana* produces protoapigenone [57–60] that has been reported to exhibit significant antitumor activity against lung cancer cells (A549) [61], liver cancer cells (Hep G2 and Hep 3B) [58], and breast cancer cells (MCF-7 [62] and MDA-MB-231) [61] with $IC_{50}$ values ranging from 0.23 to 3.88 μM [63,64]. The novel flavone protoapigenone has been reported to decrease cancer cell viability through the induction of apoptosis [65,66]. Furthermore, it has exhibited significant anticancer activity in a nude mouse model explanted with human ovarian and prostate cancer cells [65–67].

Raqui-Raqui (*Thelypteris glandulosolanosa*) is a species of fern. A review of PubMed and EMBASE does not demonstrate peer-reviewed publications with biomedical applications to date. However, its similarity to *Thelypteris torresiana* would suggest that bioactive compounds with potential anti-tumor activity are likely possible. Other ferns that belong to the *Thelypteris* genus have been studied such as *Thelypteris normalis* that contains various allelopathic compounds such as thelypterin A and B [68], the presence of the anthelmintic and fungicide benzimidazole in *Thelypteris felix-mas* [69], and the content of various drimane-type sesquiterpenoids in *Thelypteris hispidula* (Decne.) Reed [70,71]. The *Thelypteris palustris* has been used for arsenic and other heavy metal uptake phytoremediation [72–75].

The potential of plant-based nanoparticles to treat different cancers is being extensively studied and well reviewed [76] and the application of silver and gold nanoparticles to treat cancers is a very active area of research investigations [76–80]. Recent studies revealed that the use of the various metallic nanoparticles in medical sciences has various applications, such as bio-imaging [81–84], bio-sensing [85–87], and drug delivery [88–90] of nutraceuticals [23,26,91–99], and pharmaceuticals [17,20,31,100], which could affect disposition [13,24,25,27–30,32,33,101–117], lymphatic transport [118], ophthalmic drug delivery [119], and toxicity [16,19,120–122]. Often, various chemical and physical methods used for the preparation and syntheses of nanoparticles involve hazardous and toxic chemicals [123], high-cost laboratory apparatus and infrastructure [124,125], as well as capabilities of varying conditions such as temperature and high pressure [126]. Recently, a new biological approach has been developed for nanoparticle synthesis, which utilizes organic material to reduce bioactive agents isolated from plants [127–129]. These biotechnologies have low cost and are environmentally safe compared to other chemical and physical processes [130].

Our research group has previously synthesized and characterized functionalized cotton fabric with silver nanoparticles and carboxymethyl chitosan (AgNPs-CMC) [131,132]. The nanocomposite obtained from the complex [Ag $(NH_3)_2$] + was synthesized under similar conditions and verified the formation of silver nanoparticles [131]. Our results, as characterized by Dynamic Light Scattering (DLS) for $AgNO_3$, revealed a monodisperse distribution of the nanocomposite with an average hydrodynamic size of 166.7 nm [131]. Fourier Transformation Infrared spectroscopy (FT-IR) demonstrated the inhibition of spec-

tral bands at 879 and 723 $cm^{-1}$ indicating the presence of AgNPs in the nanocomposite [131]. Scanning electron microscopy (SEM) demonstrated that the silver nanoparticles were spherical in shape and between 5 and 20 nm [131]. The functionalized fabric evaluated using X-ray diffraction (XRD) analysis further confirmed the presence of silver nanoparticles [132]. Inductively Coupled Plasma Optical Emission Spectrometry (ICP-OES) determined an average concentration of 13.5 mg of silver per kg of functionalized fabric [132]. IR reported that the functionalized fabric variation had a displaced peak of intensity at 1594.32 $cm^{-1}$, corresponding to carboxylate anions [132]. Similarly, Raman spectroscopy demonstrated an intense peak at 1592.84 $cm^{-1}$, which is characteristic and corresponds to the primary amino group of carboxymethyl chitosan, and a peak at 1371.5 $cm^{-1}$ corresponding to the carboxylic anions [132]. Finally, the physical and mechanical tests of tensile strength and color index were similar [132]. The functionalized fabric possessed antimicrobial and antifungal properties against *Escherichia coli*, *Staphylococcus aureus*, *Candida albicans,* and *Aspergillus niger* [133].

Our current study is novel as it constitutes the first study of a cost-effective, eco-friendly, and convenient and facile protocol for green synthesis of AgNPs from *Thelypteris glandulosolanosa* (Raqui-raqui) leaves extract. The green synthesis methodology has recently received significant scientific attention because of its cost-effectiveness and because it is an eco-friendly technique [134–137]. Organic synthesis using various plant extracts has been previously reported in green synthesis, increasing the stability and efficiency of these nanoparticles [138–140]. The properties and efficiency of silver nanoparticles (AgNPs) depend on their morphological characteristics such as size, shape, surface area, and the type of the plant used for the synthesis of these nanoparticles [56,141]. Silver nanoparticles (AgNPs) synthesized by the biological method using *Anthemis atropatana* and *Albizia adianthifolia* have been shown to exhibit antiproliferative effects against many cancer cells [142–145]. However, the synthesis of silver nanoparticles using the aqueous extract of *Thelypteris glandulosolanosa* has not been reported and published in the literature to the best of our knowledge and review. Therefore, this study aimed to investigate the anti-cancer activity of silver nanoparticles (AgNPs) green synthesized using the aqueous extract of the *Thelypteris glandulosolanosa* on the MCF-7 breast cancer and A549 lung cancer cell lines.

The materials and methods are presented in Section 2. Section 3 provides the outcomes and discussion. Conclusions are described in Section 4.

## 2. Materials and Methods

### *2.1. Reagents and Materials*

The following reagents were used: silver nitrate (Merck Millipore, Burlington, MA, USA) and methyl thiazolyl diphenyl-tetrazolium bromide (MTT) (Merck Millipore, Burlington, MA, USA).

### *2.2. Equipment*

UV-Visible spectrophotometer (Gold Spectrum lab 54S), dynamic light scattering (DLS, Zetasizer Nano ZS), and scanning transmission electron microscopy (JEOL 2200FS STEM, with hexapolar corrector CEOS).

### *2.3. Preparation of Plant Extract of Thelypteris glandulosolanosa (Raqui-Raqui), Green Synthesis, and Purification of Silver Nanoparticles with Raqui-Raqui (AgNPs-RR)*

Green leaves of *Thelypteris glandulosolanosa* were harvested from the district of Pocsi located in the province and department of Arequipa, Peru, located at 3043 m elevation. Leaves were washed three times using distilled water then washed with Milli-Q water. All the water was removed, and the leaves were sprayed. The leaves sprayed (15 g) were first boiled with 100 mL of Milli-Q water. After cooling to room temperature, the plant extract was filtered through Whatman N°1 filter paper (particle retention: 11 um; filtration speed (Herzberg): 150 s; weight: 87 $g/m^2$) followed by filtration in Millex-GP Syringe Filter Unit, 0.22 µm (33 mm diameter sterile syringe filter with a 0.22 µm pore size hydrophilic

Polyethersulfone membrane). After filtration, the extract was stored at 4 °C for further experiments.

Silver nitrate solutions (0.1 M, $AgNO_3$) were also freshly prepared in Milli-Q water under dark conditions as previously described [146]. A range of concentrations of aqueous leaf extracts (5.00, 2.00, 1.00, 0.5, 0.2, 0.1, and 0.05% *w*/*v*) were used for the reduction of Ag into $Ag^0$ state by mixing it with 0.5 mM $AgNO_3$. These mixtures of plant extract and $AgNO_3$ were temperature controlled under 50 °C with continuous stirring. The reduction of Ag ions in solution was monitored by a visible color change and periodic mixture sampling by measuring in the UV-Visible Gold Spectrum lab 54S (λ 300 to 700 nm). The *AgNPs-RR* were centrifuged at 12,500 rpm by 15 min, washed three times with Milli-Q water, and finally washed with ethanol. The resulting *AgNPs-RR* were dried at 40 °C for 48 h.

### 2.4. Characterization of AgNPs-RR

The *AgNPs-RR* were characterized to identify their size, shape, surface area, and dispersity. The techniques used in this study to characterize nanoparticles were UV-Visible Spectra, dynamic light scattering (DLS), and scanning transmission electron microscopy (STEM).

#### 2.4.1. UV-Visible Spectra Analysis of *AgNPs-RR*

The reduction of $Ag^+$ ions and formation of *AgNPs-RR* was monitored by measuring the UV-Visible Spectra of the reaction through a spectrophotometer (Gold Spectrum lab 54S, Rinch Industrial Co., Shanghai, China) at the wavelength range of 300–700 nm (with intervals of 1 nm) using quartz cuvettes. The progress in reducing $Ag^+$ ions was monitored by a periodical sampling of the reaction mixture at different reaction times between 0, 15, 30, 45, and 90 min.

#### 2.4.2. DLS and STEM Analysis of *AgNPs-RR*

The distribution of the size of *AgNPs-RR* was analyzed by DLS (Zetasizer Nano ZS, Malvern, Worcestershire, UK), and the size of nanoparticle was available in the scanning transmission electron microscopy (JEOL 2200FS STEM, with hexapolar corrector CEOS GmbH, Heidelberg, Germany). The STEM sample was prepared by a drop of reaction sample on the copper-coated grid, and the excess of the solution was removed by drying under a mercury lamp for 5 min as previously described [147].

### 2.5. Cytotoxicity Assay

MCF-7, A549, and L929 cells were seeded into 96-well plates ($1 \times 10^5$ cells/well) and incubated with various concentrations of silver nanoparticles (AgNPs) and silver nanoparticles with Raqui-Raqui (*AgNPs-RR*) (100, 50, 25, 12.5, 6.25, 3.12, 1.56, and 0.78 μg/mL) for 48 h at 37 °C in 5% $CO_2$ humidified incubator. The cytotoxic activity was measured by a methyl thiazolyl diphenyl-tetrazolium bromide (MTT) assay and cell viability percentage was calculated by optical density values subjected in the formula as previously described [148,149].

### 2.6. Statistical Analysis

All data is represented as mean ± S.E. The statistical analysis was carried out with GraphPad Version 6.01 using one-way ANOVA, statistical significance was examined by Tukey's post hoc with statistical significance at $p$-values < 0.05.

## 3. Results and Discussion

### 3.1. UV-Visible Spectra Analysis of AgNPs and AgNPs-RR

In this work, the green synthesis of *AgNPs-RR* was performed using different concentrations (5, 2, 1, 0.5, 0.2, 0.1, and 0.05%) of an aqueous extract of *Thelypteris glandulosolanosa* (Raqui-Raqui) in a 1:3 stochiometric relationship as a reduction agent for silver nitrate (0.5 mM). When the colorless solution of $AgNO_3$ was mixed with Raqui-Raqui,

the bathochromic shift in wavelength maximum and change from colorless to intense yellow indicated the synthesis of *AgNPs-RR*. UV-Visible further attested to the formation of this nanoparticle, where the broad peak was observed between 420 and 450 nm. In our results, maximum absorption was observed at 450 nm. Although, the spectra were registered at different reaction time intervals, a peak at 420 nm was revealed and reproducible at 0.5% concentration, which suggested that the formed nanoparticles were stable and polydispersed (Figure 1).

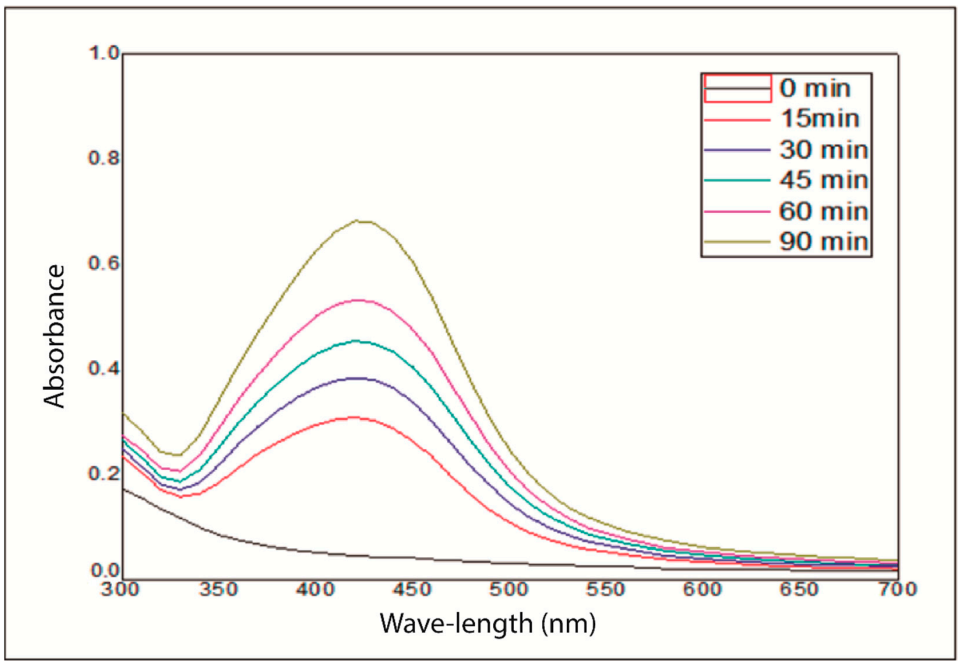


**Figure 1.** Absorbance of *AgNPs-RR*.

Kumara Swamy et al. observed the formation of AgNPs at 1 h of incubation with an aqueous extract of *Leptadenia reticulata* [150]. Furthermore, color changes of the reaction mixture have been reported by a reduction of $AgNO_3$ by the aqueous extract of *Albizia saman* leaf [151]. Additionally, the extract of *Eclipta alba* leaves has been reported to reduce silver ions to silver nanoparticles [152]. An increment of color intensity and surface plasmon resonance (SPR) band sharpness have been reported to indicate the reduction of $Ag^+$ into $Ag^0$ [153]. Additionally, to verify the formation of the AgNPs, the researchers carried out an analysis in a UV-visible spectrophotometer [153]. The analysis showed maximum absorbance close to 420 and 411 nm [153], which is similar to the results in our study. The lack of similarity in observed bioreduction rates is likely a function of leaf extracts from different plant species used as reducing and stabilizing agents. Therefore, the current study contributes to identifying a potential new plant species for the synthesis of silver nanoparticles such as *Thelypteris glandulosolanosa* (Raqui-Raqui).

### *3.2. DLS Analysis of AgNPs-RR*

The dynamic light scattering (DLS) analysis was carried out in an aqueous solution to determine the average hydrodynamic size of the *AgNPs-RR*. Figure 2 shows the size distribution, with a Z-average (d.nm) of 48.11 and polydispersity of 0.472. A characteristic bimodal distribution of nanoparticles is apparent which suggests the possibility of agglomeration in solution (peak 2, 258.1 ± 133.5 nm). A more significant part of the extract was incorporated in the AgNPs (peak 1, 39.16 ± 18.49 nm; peak 3, 7.99 ± 1.06 nm). The area under the curve expresses the proportion of each fraction of AgNPs in the solution, so fraction 1 corresponding to 39.16 ± 18.49 nm presents a more significant proportion of the extract of Raqui-Raqui incorporated in the nanoparticles [154–156]. In contrast, Arya

et al. reported that the average hydrodynamic size of the silver nanoparticles determined by DLS is approximately 54.00 nm [153]. An index polydispersion of 0.2 was reported to the AgNPs biosynthesized using bark extract of Prosopis juliflora indicating that they were homogeneous in size [153]. The polydispersity index (PDI) is the ratio of mass average molecular mass to the number average molecular mass (PDI = MnMw). PDI is used as a measure of broadness of molecular weight distribution. The PDI is a measure of the heterogeneity of a sample based on size. Polydispersity can occur due to size distribution in a sample or agglomeration or aggregation of the sample during isolation or analysis. PDI values < 0.05 are more common to monodisperse samples, while values > 0.7 are common to a broad size (e.g., polydisperse) distribution of particles. The numerical value of PDI ranges from 0.0 (for a perfectly uniform sample with respect to the particle size) to 1.0 (for a highly polydisperse sample with multiple particle size populations) [157]. The PDI was determined to be 0.472. There is no general limit for acceptable polydispersity. In Quality by Design for manufacturing, PDI may or may not be critical for a specification. ISO silver nanoparticles suggest AgNPs with PDI less than 0.5 or 0.1 are considered to be monodisperse and might have less aggregation. AgNPs with PDI > 0.7 or equal to 1 are considered to be polydispersed and might aggregate.

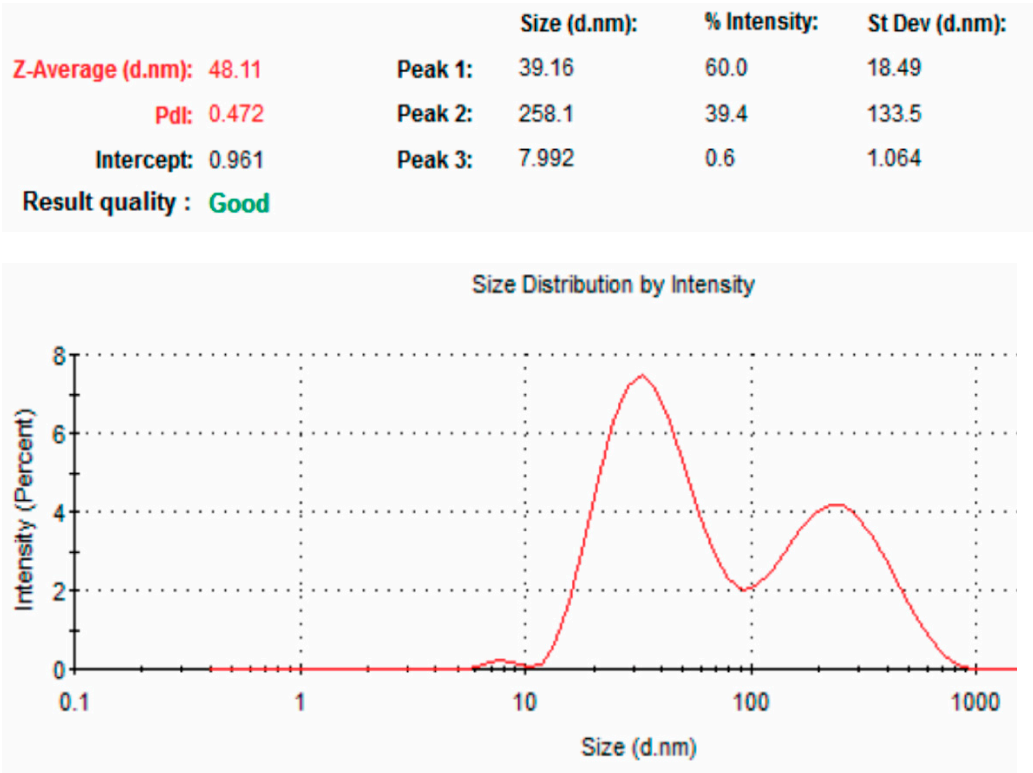


**Figure 2.** Size distribution of *AgNPs-RR* using dynamic light scattering (DLS).

Similarly, Remya et al. reported that the analysis in DLS of the nanoparticles biologically synthesized using the aqueous extract of flower of *Cassia fistula* showed polydisperse nanoparticles with average size between 21.00 and 30.00 nm [158]. Likewise, Kim et al. reported the particle size distribution analysis by DLS, which comprised a 50–150 nm size range and hydrodynamic diameter of 97 nm with an average size and shape of the nanoparticles confirmed and paralleled the findings obtained from scanning electron microscopy (STEM) analysis [159].

### *3.3. STEM Analysis of AgNPs-RR*

Images of the surface size of the purified *AgNPs-RR* were examined using scanning transmission electron microscopy (STEM). For the analysis, the purified sample was dis-

persed by ultrasound in ethanol to form very dilute suspensions and then STEM images of the drops deposited on the coated copper grids carbon were obtained. The *AgNPs-RR* purified exhibited a quasi-spherical shape and showed aggregation and polydispersity (Figure 3A,B). The size distribution was analyzed using the software ImageJ. The nanoparticles presented a size distribution of 6.64–51.00 nm and an average diameter of 31.45 nm (Figure 3C). This result is similar and is in agreement with the analysis proposed by Jha et al., who reported that the biologically synthesized nanoparticles were spherical and their size ranged between 2 and 50 nm [160]. The average size of the *AgNPs-RR* analyzed by STEM was smaller than that analyzed by DLS (31.45 nm vs. 48.11 nm). STEM is a direct method of particle size analysis while DLS is an indirect method [154–156]. Differences in methods of analysis from the STEM samples which were evaluated from a dry non-hydrated state that are individually isolated, and the measurement obtained was the surface size of the nanoparticles; on the other hand, DLS evaluates the hydrodynamic size in suspension accounting for an increase in small mean particle size difference between characterization methodology.

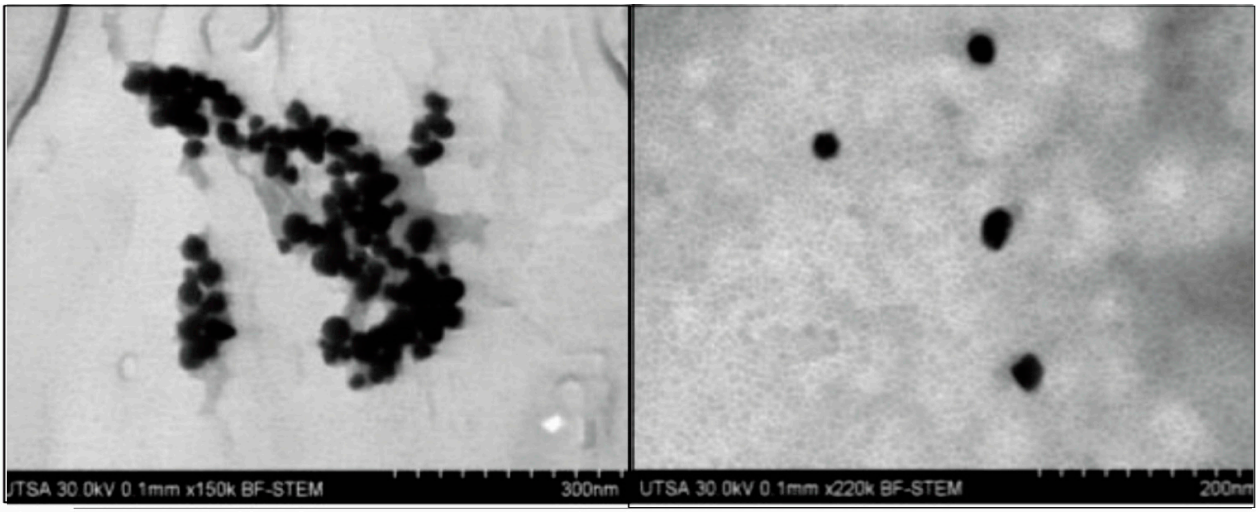


(**A**) (**B**)

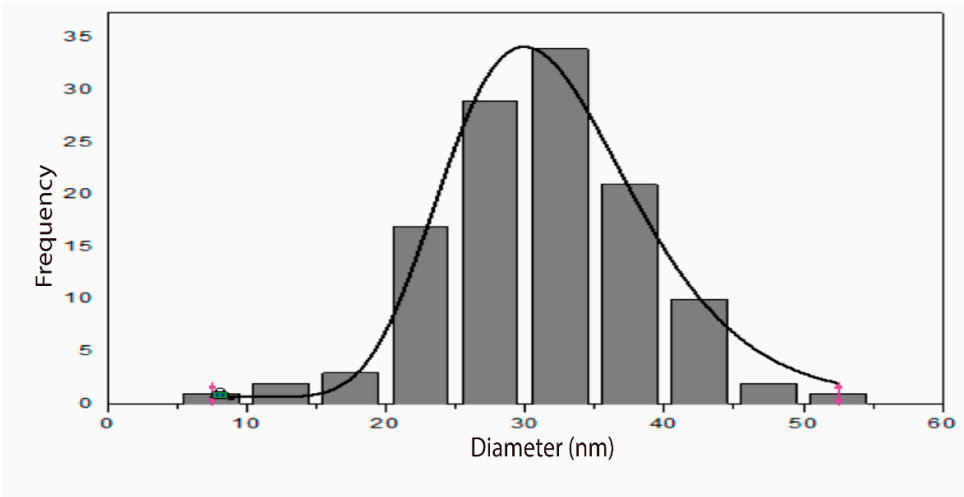


(**C**)

**Figure 3.** Left (**A**) Image of *AgNPs-RR* using scanning transmission electron microscopy (STEM). Right (**B**) Zoomed image of single *AgNPs-RR* using STEM. (**C**) Size distribution of *AgNPs-RR*.

### *3.4. Cell Toxicity of AgNPs-RR in L929, A549, and MC-F7 Cell Lines*

Previous reports suggested that green synthesized AgNPs have greater capacity to suppress cancerous cell growth and have potential for further anti-cancer development as a nanotherapeutic [161–164]. In this work, we examined the cytotoxicity of AgNPs and *AgNPs-RR* through MTT assay and we observed that the percentage of cell viability decreased dose-dependently with increasing concentration of AgNPs and *AgNPs-RR* (Figure 4), and the $IC_{50}$ value was observed at 12.50 μg/mL for the A549 and MCF7 cell lines.

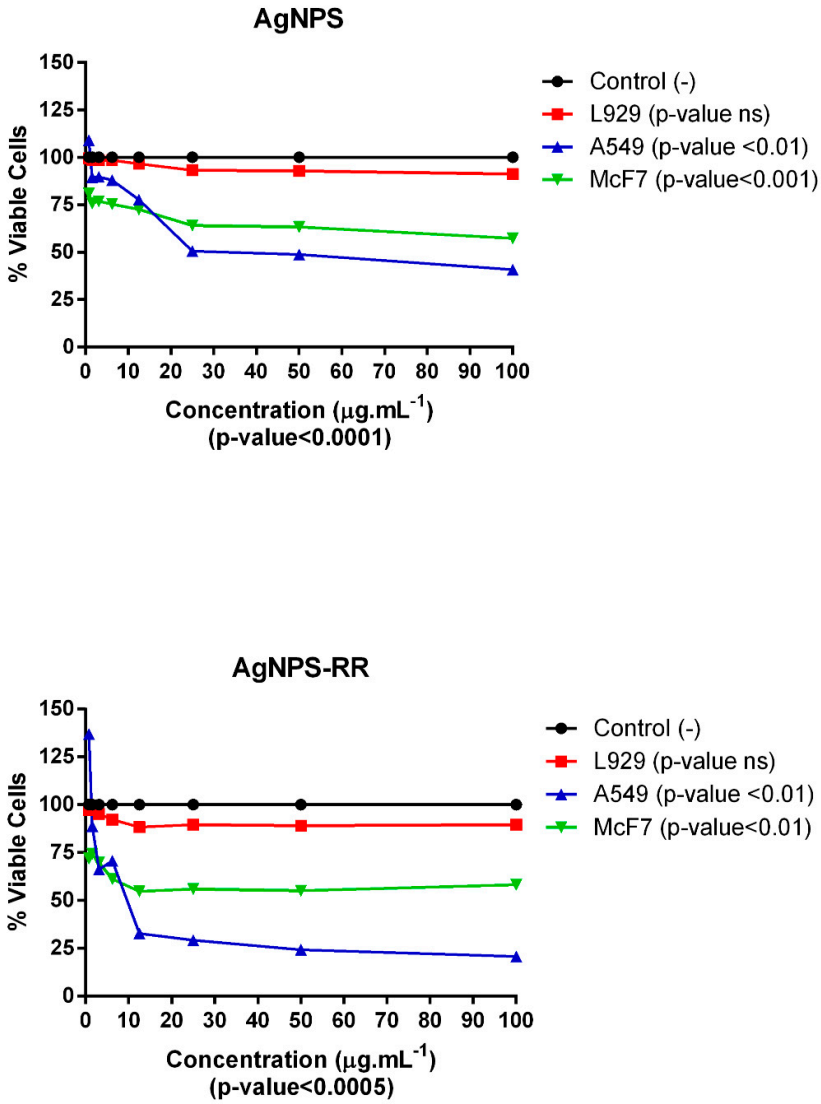


**Figure 4.** Cell viability with AgNPs and *AgNPs-RR*.

The *AgNPs-RR* had no apparent cytotoxic to the L929 cell line. Similar dose-dependent responses of AgNPs were reported in a HCT15 cell line with a green synthesis of *Vitex negundo* [161], in SiHa (human hyper-triploid cervical carcinoma cell line) with green synthesis of *Withania coagulans* [147] and in human cervical carcinoma cells with green synthesis of *Podophyllum hexandrum* [165]. Among various species of ferns, *Thelypteris torresiana* produces protoapigenone that exhibits significant antitumor activity against lung cancer cells (A549) [61], liver cancer cells (Hep G2 and Hep 3B) [58], and breast cancer cells (MCF-7 [62] and MDA-MB-231) [61] with $IC_{50}$ values ranging from 0.23 to 3.88 μM [10]. Chang et al. showed that this novel flavone decreased cancer cells viability through the induction of apoptosis [65]. Furthermore, protoapigenone exhibited significant anti-cancer activity in a nude mouse inoculated with human ovarian and prostate cancer cells [65–67].

In our research, we observed the $IC_{50}$ at 12.50 μg/mL in the same cellular strains used by Chen et al. [65], Chang et al. [66], and Lin et al. [67]. However, previous studies assessed the activity of protoapigenone extracted from *Thelypteris torresiana*, while we worked with a full aqueous extract of Raqui-Raqui. Ultimately, in vivo detoxification of nanoparticles from a patient's body is critical for safe and effective nano-based therapy [120]. Filtration and total body clearance of AgNPs from the systemic circulation of cancer patients treated with metallic nanoparticles needs further investigation to minimize cell cytotoxicity as outlined previously [165].

## 4. Conclusions

A preliminary study of the potential eco-friendly, cost-effective, and convenient green synthesis of novel silver nanoparticles using an aqueous extract of *Thelypteris glandulosolanosa* (Raqui-Raqui) leaves was undertaken. The *AgNPs-RR* exhibited properties to reduce $AgNO_3$ solution, an average size of 39.16 nm using DLS analysis and 31.45 nm using STEM analysis. Synthesized AgNPs demonstrated cytotoxicity against cancer cells (A549 and MCF7) and were not cytotoxic in non-cancerous cells. Additional physicochemical characterization studies to further elucidate the particles and follow up biological studies to understand the mechanisms of action of *AgNPs-RR* and their potential applications and development as delivery systems in vivo are required.

**Author Contributions:** Conceptualization, L.D.C.V.-N., J.O.C.-R., C.A.A.-C., L.M.d.H., C.V.-G.; methodology, L.D.C.V.-N., J.O.C.-R., C.A.A.-C., L.M.d.H., C.V.-G.; software, L.D.C.V.-N., J.O.C.-R., C.A.A.-C., L.M.d.H., C.V.-G.; validation, L.D.C.V.-N., J.O.C.-R., C.A.A.-C., L.M.d.H., C.V.-G.; formal analysis, L.D.C.V.-N., J.O.C.-R., C.A.A.-C., L.M.d.H., C.V.-G., N.M.D., J.A.Y.; investigation, L.D.C.V.-N., J.O.C.-R., C.A.A.-C., L.M.d.H., C.V.-G.; resources, L.D.C.V.-N., J.O.C.-R., C.A.A.-C., L.M.d.H., C.V.-G.; data curation, L.D.C.V.-N., J.O.C.-R., C.A.A.-C., L.M.d.H., C.V.-G.; writing—original draft preparation, L.D.C.V.-N., J.O.C.-R., C.A.A.-C., L.M.d.H., C.V.-G., A.A.-R., S.D.-A.-A., N.M.D., J.A.Y.; writing—review and editing, L.D.C.V.-N., J.O.C.-R., C.A.A.-C., L.M.d.H., C.V.-G., A.A.-R., S.D.-A.-A., N.M.D., J.A.Y.; visualization, L.D.C.V.-N., J.O.C.-R., C.A.A.-C., L.M.d.H., C.V.-G., A.A.-R., S.D.-A.-A., N.M.D., J.A.Y. All authors have read and agreed to the published version of the manuscript.

**Funding:** This research received no external funding.

**Data Availability Statement:** The data presented in this study are available on request from the corresponding author.

**Conflicts of Interest:** The authors declare no conflict of interest.

## References

1. Bray, F.; Ferlay, J.; Soerjomataram, I.; Siegel, R.L.; Torre, L.A.; Jemal, A. Global cancer statistics 2018: GLOBOCAN estimates of incidence and mortality worldwide for 36 cancers in 185 countries. *CA A Cancer J. Clin.* **2018**, *68*, 394–424. [CrossRef] [PubMed]
2. Tian, Y.; Wang, Z.; Liu, X.; Duan, J.; Feng, G.; Yin, Y.; Gu, J.; Chen, Z.; Gao, S.; Bai, H.; et al. Prediction of Chemotherapeutic Efficacy in Non–Small Cell Lung Cancer by Serum Metabolomic Profiling. *Clin. Cancer Res.* **2018**, *24*, 2100–2109. [CrossRef] [PubMed]
3. Waks, A.G.; Winer, E.P. Breast Cancer Treatment: A Review. *JAMA* **2019**, *321*, 288–300. [CrossRef] [PubMed]
4. Torre, L.A.; Bray, F.; Siegel, R.L.; Ferlay, J.; Lortet-Tieulent, J.; Jemal, A. Global cancer statistics, 2012. *CA A Cancer J. Clin.* **2015**, *65*, 87–108. [CrossRef]
5. Ferlay, J.; Colombet, M.; Soerjomataram, I.; Parkin, D.M.; Piñeros, M.; Znaor, A.; Bray, F. Cancer statistics for the year 2020: An overview. *Int. J. Cancer* **2021**, *149*, 778–789. [CrossRef] [PubMed]
6. Siegel, R.L.; Miller, K.D.; Fuchs, H.E.; Jemal, A. Cancer statistics, 2022. *CA A Cancer J. Clin.* **2022**, *72*, 7–33. [CrossRef]
7. Dang, Y.; Guan, J. Nanoparticle-based drug delivery systems for cancer therapy. *Smart Mater. Med.* **2020**, *1*, 10–19. [CrossRef]
8. Telli, M.L.; Gradishar, W.J.; Ward, J.H. NCCN Guidelines Updates: Breast Cancer. *J. Natl. Compr. Cancer Netw.* **2019**, *17*, 552–555. [CrossRef]
9. Waks, A.G.; Winer, E.P. Breast Cancer Treatment. *JAMA* **2019**, *321*, 316. [CrossRef]
10. Gennari, A.; André, F.; Barrios, C.H.; Cortés, J.; de Azambuja, E.; DeMichele, A.; Dent, R.; Fenlon, D.; Gligorov, J.; Hurvitz, S.A.; et al. ESMO Clinical Practice Guideline for the diagnosis, staging and treatment of patients with metastatic breast cancer. *Ann. Oncol.* **2021**, *32*, 1475–1495. [CrossRef]
11. Goldstein, M.; Kastan, M.B. The DNA Damage Response: Implications for Tumor Responses to Radiation and Chemotherapy. *Annu. Rev. Med.* **2015**, *66*, 129–143. [CrossRef] [PubMed]

12. DeMario, M.D.; Ratain, M.J. Oral chemotherapy: Rationale and future directions. *J. Clin. Oncol.* **1998**, *16*, 2557–2567. [CrossRef] [PubMed]
13. Alrushaid, S.; Davies, N.M.; Anderson, J.E.; Le, T.; Yáñez, J.A.; Maayah, Z.H.; El-Kadi, A.O.S.; Rachid, O.; Sayre, C.L.; Löbenberg, R.; et al. Pharmaceutical characterization of myonovin, a novel skeletal muscle regenerator: In silico, in vitro and in vivo studies. *J. Pharm. Pharm. Sci.* **2018**, *21*, 1s–18s. [CrossRef]
14. Freyer, G.; Ligneau, B.; Tranchand, B.; Ardiet, C.; Serre-Debeauvais, F.; Trillet-Lenoir, V. Pharmacokinetic studies in cancer chemotherapy: Usefulness in clinical practice. *Cancer Treat. Rev.* **1997**, *23*, 153–169. [CrossRef]
15. Pagani, M.; Bavbek, S.; Alvarez-Cuesta, E.; Berna Dursun, A.; Bonadonna, P.; Castells, M.; Cernadas, J.; Chiriac, A.; Sahar, H.; Madrigal-Burgaleta, R.; et al. Hypersensitivity reactions to chemotherapy: An EAACI Position Paper. *Allergy* **2022**, *77*, 388–403. [CrossRef] [PubMed]
16. Bonin, A.M.; Yáñez, J.A.; Fukuda, C.; Teng, X.W.; Dillon, C.T.; Hambley, T.W.; Lay, P.A.; Davies, N.M. Inhibition of experimental colorectal cancer and reduction in renal and gastrointestinal toxicities by copper-indomethacin in rats. *Cancer Chemother. Pharmacol.* **2010**, *66*, 755–764. [CrossRef]
17. Yanez, J.A.; Forrest, M.L.; Ohgami, Y.; Kwon, G.S.; Davies, N.M. Pharmacometrics and delivery of novel nanoformulated PEG-b-poly(epsilon-caprolactone) micelles of rapamycin. *Cancer Chemother. Pharmacol.* **2008**, *61*, 133–144. [CrossRef] [PubMed]
18. Wauthoz, N.; Rosière, R.; Amighi, K. Inhaled cytotoxic chemotherapy: Clinical challenges, recent developments, and future prospects. *Expert Opin. Drug Deliv.* **2021**, *18*, 333–354. [CrossRef]
19. Alrushaid, S.; Sayre, C.L.; Yáñez, J.A.; Forrest, M.L.; Senadheera, S.N.; Burczynski, F.J.; Löbenberg, R.; Davies, N.M. Pharmacokinetic and Toxicodynamic Characterization of a Novel Doxorubicin Derivative. *Pharmaceutics* **2017**, *9*, 35. [CrossRef]
20. Xiong, M.P.; Yanez, J.A.; Remsberg, C.M.; Ohgami, Y.; Kwon, G.S.; Davies, N.M.; Forrest, M.L. Formulation of a geldanamycin prodrug in mPEG-b-PCL micelles greatly enhances tolerability and pharmacokinetics in rats. *J. Control. Release* **2008**, *129*, 33–40. [CrossRef]
21. Jahangirian, H.; Kalantari, K.; Izadiyan, Z.; Rafiee-Moghaddam, R.; Shameli, K.; Webster, T.J. A review of small molecules and drug delivery applications using gold and iron nanoparticles. *Int. J. Nanomed.* **2019**, *14*, 1633–1657. [CrossRef]
22. Mangal, S.; Gao, W.; Li, T.; Zhou, Q. Pulmonary delivery of nanoparticle chemotherapy for the treatment of lung cancers: Challenges and opportunities. *Acta Pharmacol. Sin.* **2017**, *38*, 782–797. [CrossRef] [PubMed]
23. Bermudez-Aguirre, D.; Yáñez, J.; Dunne, C.; Davies, N.; Barbosa-Cánovas, G. Study of strawberry flavored milk under pulsed electric field processing. *Food Res. Int.* **2010**, *43*, 2201–2207. [CrossRef]
24. Yáñez, J.A.; Miranda, N.D.; Remsberg, C.M.; Ohgami, Y.; Davies, N.M. Stereospecific high-performance liquid chromatographic analysis of eriodictyol in urine. *J. Pharm. Biomed. Anal.* **2007**, *43*, 255–262. [CrossRef]
25. Vega-Villa, K.R.; Remsberg, C.M.; Ohgami, Y.; Yanez, J.A.; Takemoto, J.K.; Andrews, P.K.; Davies, N.M. Stereospecific high-performance liquid chromatography of taxifolin, applications in pharmacokinetics, and determination in tu fu ling (Rhizoma smilacis glabrae) and apple (Malus x domestica). *Biomed. Chromatogr.* **2009**, *23*, 638–646. [CrossRef]
26. Ramos-Escudero, F.; Santos-Buelga, C.; Pérez-Alonso, J.J.; Yáñez, J.A.; Dueñas, M. HPLC-DAD-ESI/MS identification of anthocyanins in Dioscorea trifida L. yam tubers (purple sachapapa). *Eur. Food Res. Technol.* **2010**, *230*, 745–752. [CrossRef]
27. Roupe, K.A.; Helms, G.L.; Halls, S.C.; Yanez, J.A.; Davies, N.M. Preparative enzymatic synthesis and HPLC analysis of rhapontigenin: Applications to metabolism, pharmacokinetics and anti-cancer studies. *J. Pharm. Pharm. Sci.* **2005**, *8*, 374–386.
28. Yáñez, J.A.; Remsberg, C.M.; Takemoto, J.K.; Vega-Villa, K.R.; Andrews, P.K.; Sayre, C.L.; Martinez, S.E.; Davies, N.M. Polyphenols and Flavonoids: An Overview. In *Flavonoid Pharmacokinetics: Methods of Analysis, Preclinical and Clinical Pharmacokinetics, Safety, and Toxicology*; Davies, N.M., Yáñez, J.A., Eds.; John Wiley & Sons: Hoboken, NJ, USA, 2012; pp. 1–69.
29. Yáñez, J.A.; Teng, X.W.; Roupe, K.A.; Davies, N.M. Stereospecific high-performance liquid chromatographic analysis of hesperetin in biological matrices. *J. Pharm. Biomed. Anal.* **2005**, *37*, 591–595. [CrossRef]
30. Remsberg, C.M.; Yanez, J.A.; Roupe, K.A.; Davies, N.M. High-performance liquid chromatographic analysis of pterostilbene in biological fluids using fluorescence detection. *J. Pharm. Biomed. Anal.* **2007**, *43*, 250–254. [CrossRef]
31. Xiong, M.P.; Yáñez, J.A.; Kwon, G.S.; Davies, N.M.; Forrest, M.L. A cremophor-free formulation for tanespimycin (17-AAG) using PEO-b-PDLLA micelles: Characterization and pharmacokinetics in rats. *J. Pharm. Sci.* **2009**, *98*, 1577–1586. [CrossRef]
32. Yanez, J.A.; Davies, N.M. Stereospecific high-performance liquid chromatographic analysis of naringenin in urine. *J. Pharm. Biomed. Anal.* **2005**, *39*, 164–169. [CrossRef]
33. Remsberg, C.M.; Yanez, J.A.; Ohgami, Y.; Vega-Villa, K.R.; Rimando, A.M.; Davies, N.M. Pharmacometrics of pterostilbene: Preclinical pharmacokinetics and metabolism, anticancer, antiinflammatory, antioxidant and analgesic activity. *Phytother. Res.* **2008**, *22*, 169–179. [CrossRef]
34. Demain, A.L.; Vaishnav, P. Natural products for cancer chemotherapy. *Microb. Biotechnol.* **2011**, *4*, 687–699. [CrossRef]
35. Vemuri, S.K.; Banala, R.R.; Mukherjee, S.; Uppula, P.; Subbaiah, G.P.V.; AV, G.R.; Malarvilli, T. Novel biosynthesized gold nanoparticles as anti-cancer agents against breast cancer: Synthesis, biological evaluation, molecular modelling studies. *Mater. Sci. Eng. C* **2019**, *99*, 417–429. [CrossRef]
36. Sureshkumar, J.; Silambarasan, R.; Bharati, K.A.; Krupa, J.; Amalraj, S.; Ayyanar, M. A review on ethnomedicinally important pteridophytes of India. *J. Ethnopharmacol.* **2018**, *219*, 269–287. [CrossRef]
37. Kumar, S.V.; Kanwar, S. Medicinal Pteridophytes Used in the Treatment of Various Diseases by the Inhabitants of Sarkaghat Tehsil, Mandi District, Himachal Pradesh. *J. Pharm. Sci. Res.* **2020**, *12*, 360–364.

38. Ozturk, M.; Altay, V.; Latıff, A.; Salman, T.; Choudhry, I. A Comparative Analysis of the Medicinal Pteridophytes in Turkey, Pakistan, and Malaysia. In *Plant and Human Health, Volume 1: Ethnobotany and Physiology*; Ozturk, M., Hakeem, K.R., Eds.; Springer International Publishing: Cham, Switzerland, 2018; pp. 349–390.
39. Bhattarai, S.; Kunwar, R.M. Nepalese Pteridophytes Used as Antimicrobials: Challenges and Opportunities. In *Promising Antimicrobials from Natural Products*; Rai, M., Kosalec, I., Eds.; Springer International Publishing: Cham, Switzerland, 2022; pp. 15–30.
40. Haq, F. Multivariate statistical analysis of pteridophytes diversity in the Sino-Japanese territory. A case study from Battagram District. *Acta Ecol. Sin.* **2022**. [CrossRef]
41. Gonzales de la Cruz, M.; Baldeón Malpartida, S.; Beltrán Santiago, H.; Jullian, V.; Bourdy, G. Hot and cold: Medicinal plant uses in Quechua speaking communities in the high Andes (Callejón de Huaylas, Ancash, Perú). *J. Ethnopharmacol.* **2014**, *155*, 1093–1117. [CrossRef]
42. Tryon, A.F. Ferns of the Incas. *Am. Fern J.* **1959**, *49*, 10–24. [CrossRef]
43. Reinaldo, R.C.P.d.S.; Santiago, A.C.P.; Medeiros, P.M.; Albuquerque, U.P. Do ferns and lycophytes function as medicinal plants? A study of their low representation in traditional pharmacopoeias. *J. Ethnopharmacol.* **2015**, *175*, 39–47. [CrossRef]
44. Bussmann, R.W.; Sharon, D. Shadows of the colonial past—diverging plant use in Northern Peru and Southern Ecuador. *J. Ethnobiol. Ethnomed.* **2009**, *5*, 4. [CrossRef] [PubMed]
45. Rastogi, S.; Pandey, M.M.; Rawat, A.K.S. Ethnopharmacological uses, phytochemistry and pharmacology of genus Adiantum: A comprehensive review. *J. Ethnopharmacol.* **2018**, *215*, 101–119. [CrossRef] [PubMed]
46. Chang, H.-C.; Gupta, S.K.; Tsay, H.-S. Studies on Folk Medicinal Fern: An Example of "Gu-Sui-Bu". In *Working with Ferns: Issues and Applications*; Kumar, A., Fernández, H., Revilla, M.A., Eds.; Springer New York: New York, NY, USA, 2010; pp. 285–304.
47. Vetter, J. Secondary Metabolites of Ferns. In *Current Advances in Fern Research*; Fernández, H., Ed.; Springer International Publishing: Cham, Switzerland, 2018; pp. 305–327.
48. Santhosh, P.; Nithya, T.G.; Lakshmi, S.G.; Marino, G.L.S.; Balavaishnavi, B.; Kamaraj, M. Assessment of phytochemicals, antioxidant, antibacterial activity, and profiling of functional molecules in novel freshwater fern Salvinia cucullata Roxb. *S. Afr. J. Bot.* **2022**. [CrossRef]
49. Szypuła, W.J.; Pietrosiuk, A. Biology, Phytochemistry, Pharmacology, and Biotechnology of European Ferns, Club Mosses, and Horsetails: A Review. In *Medicinal Plants: Domestication, Biotechnology and Regional Importance*; Ekiert, H.M., Ramawat, K.G., Arora, J., Eds.; Springer International Publishing: Cham, Switzerland, 2021; pp. 605–660.
50. Johnson, M.A.; Madona, C.X.; Almeida, R.S.; Martins, N.; Coutinho, H.D.M. In Vitro Toxicity, Antioxidant, Anti-Inflammatory, and Antidiabetic Potential of *Sphaerostephanos unitus* (L.) Holttum. *Antibiotics* **2020**, *9*, 333. [CrossRef]
51. Reddy, M.N.; Adnan, M.; Alreshidi, M.M.; Saeed, M.; Patel, M. Evaluation of Anticancer, Antibacterial and Antioxidant Properties of a Medicinally Treasured Fern Tectaria coadunata with its Phytoconstituents Analysis by HR-LCMS. *Anti-Cancer Agents Med. Chem. Anti-Cancer Agents* **2020**, *20*, 1845–1856. [CrossRef]
52. Chandran, G.; Smitha Grace, S.R.; Chauhan, J.B. Fern to Pharma: Potential Neuroameliorative Properties of Pteridophytes. In *Plant and Human Health, Volume 3: Pharmacology and Therapeutic Uses*; Ozturk, M., Hakeem, K.R., Eds.; Springer International Publishing: Cham, Switzerland, 2019; pp. 195–208.
53. Tang, Y.; Fang, W.; Ma, Y.T.; Cai, Y.L.; Ruan, J.L. A novel flavonoid from the root of Macrothelypteris torresiana (Gaud.) Ching. *Chin. Chem. Lett.* **2009**, *20*, 815–816. [CrossRef]
54. Tang, Y.; Xiong, C.; Zhou, D.; Wei, A.; Fu, W.; Cai, Y.; Ruan, J. A new flavonoid from Macrothelypteris torresiana. *Chem. Nat. Compd.* **2010**, *46*, 209–211. [CrossRef]
55. Fang, W.; Ruan, J.; Cai, Y.; Wei, A.; Zhou, D.; Zhang, W. Flavonoids from the aerial parts of Macrothelypteris torresiana. *Nat. Prod. Res.* **2011**, *25*, 36–39. [CrossRef]
56. Lin, A.-S.; Chang, F.-R.; Yen, H.-F.; Bjorkeborn, H.; Norlen, P.; Wu, Y.-C. Novel Flavonoids of Thelypteris torresiana. *Chem. Pharm. Bull.* **2007**, *55*, 635–637. [CrossRef]
57. Chiu, C.-C.; Chang, H.-W.; Chuang, D.-W.; Chang, F.-R.; Chang, Y.-C.; Cheng, Y.-S.; Tsai, M.-T.; Chen, W.-Y.; Lee, S.-S.; Wang, C.-K.; et al. Fern Plant–Derived Protoapigenone Leads to DNA Damage, Apoptosis, and G2/M Arrest in Lung Cancer Cell Line H1299. *DNA Cell Biol.* **2009**, *28*, 501–506. [CrossRef]
58. Poór, M.; Li, Y.; Kunsági-Máté, S.; Varga, Z.; Hunyadi, A.; Dankó, B.; Chang, F.-R.; Wu, Y.-C.; Kőszegi, T. Protoapigenone derivatives: Albumin binding properties and effects on HepG2 cells. *J. Photochem. Photobiol. B Biol.* **2013**, *124*, 20–26. [CrossRef] [PubMed]
59. Tung, C.-P.; Chang, F.-R.; Wu, Y.-C.; Chuang, D.-W.; Hunyadi, A.; Liu, S.-T. Inhibition of the Epstein–Barr virus lytic cycle by protoapigenone. *J. Gen. Virol.* **2011**, *92*, 1760–1768. [CrossRef] [PubMed]
60. Lin, A.S.; Chang, F.R.; Wu, C.C.; Liaw, C.C.; Wu, Y.C. New cytotoxic flavonoids from Thelypteris torresiana. *Planta Med.* **2005**, *71*, 867–870. [CrossRef] [PubMed]
61. Xue, P.; Zhao, Y.; Liu, Y.; Yuan, Q.; Xiong, C.; Ruan, J. A novel compound RY10-4 induces apoptosis and inhibits invasion via inhibiting STAT3 through ERK-, p38-dependent pathways in human lung adenocarcinoma A549 cells. *Chem. Biol. Interact.* **2014**, *209*, 25–34. [CrossRef]
62. Zhang, X.; Wei, H.; Liu, Z.; Yuan, Q.; Wei, A.; Shi, D.; Yang, X.; Ruan, J. A novel protoapigenone analog RY10-4 induces breast cancer MCF-7 cell death through autophagy via the Akt/mTOR pathway. *Toxicol. Appl. Pharmacol.* **2013**, *270*, 122–128. [CrossRef]

63. Chen, W.-Y.; Hsieh, Y.-A.; Tsai, C.-I.; Kang, Y.-F.; Chang, F.-R.; Wu, Y.-C.; Wu, C.-C. Protoapigenone, a natural derivative of apigenin, induces mitogen-activated protein kinase-dependent apoptosis in human breast cancer cells associated with induction of oxidative stress and inhibition of glutathione S-transferase π. *Investig. New Drugs* **2011**, *29*, 1347–1359. [CrossRef]
64. Hunyadi, A.; Chuang, D.-W.; Danko, B.; Chiang, M.Y.; Lee, C.-L.; Wang, H.-C.; Wu, C.-C.; Chang, F.-R.; Wu, Y.-C. Direct Semi-Synthesis of the Anticancer Lead-Drug Protoapigenone from Apigenin, and Synthesis of Further New Cytotoxic Protoflavone Derivatives. *PLoS ONE* **2011**, *6*, e23922. [CrossRef]
65. Chang, H.-L.; Su, J.-H.; Yeh, Y.-T.; Lee, Y.-C.; Chen, H.-M.; Wu, Y.-C.; Yuan, S.-S.F. Protoapigenone, a novel flavonoid, inhibits ovarian cancer cell growth in vitro and in vivo. *Cancer Lett.* **2008**, *267*, 85–95. [CrossRef]
66. Chang, H.-L.; Wu, Y.-C.; Su, J.-H.; Yeh, Y.-T.; Yuan, S.-S.F. Protoapigenone, a Novel Flavonoid, Induces Apoptosis in Human Prostate Cancer Cells through Activation of p38 Mitogen-Activated Protein Kinase and c-Jun NH2-Terminal Kinase 1/2. *J. Pharmacol. Exp. Ther.* **2008**, *325*, 841. [CrossRef]
67. Lin, A.-S.; Nakagawa-Goto, K.; Chang, F.-R.; Yu, D.; Morris-Natschke, S.L.; Wu, C.-C.; Chen, S.-L.; Wu, Y.-C.; Lee, K.-H. First Total Synthesis of Protoapigenone and Its Analogues as Potent Cytotoxic Agents. *J. Med. Chem.* **2007**, *50*, 3921–3927. [CrossRef]
68. Davidonis, G.H.; Ruddat, M. Allelopathic compounds, thelypterin A and B in the fern Thelypteris normalis. *Planta* **1973**, *111*, 23–32. [CrossRef] [PubMed]
69. Dyar, J.J.; Shade, J. The Influence of Benzimidazole on the Gametophyte of Thelypteris felix-mas. *Plant Physiol.* **1974**, *53*, 666–668. [CrossRef] [PubMed]
70. Socolsky, C.; Muruaga, N.; Bardón, A. Drimanes and other terpenoids from the fern Thelypteris hispidula (Decne.) Reed. *Chem. Biodivers.* **2005**, *2*, 1105–1108. [CrossRef] [PubMed]
71. Asakawa, Y.; Ludwiczuk, A.; Harinantenaina, L.; Toyota, M.; Nishiki, M.; Bardon, A.; Nii, K. Distribution of drimane sesquiterpenoids and tocopherols in liverworts, ferns and higher plants: Polygonaceae, Canellaceae and Winteraceae species. *Nat. Prod. Commun.* **2012**, *7*, 685–692. [CrossRef] [PubMed]
72. Anderson, L.; Walsh, M.M. Arsenic uptake by common marsh fern Thelypteris palustris and its potential for phytoremediation. *Sci. Total Environ.* **2007**, *379*, 263–265. [CrossRef] [PubMed]
73. Anderson, L.L.; Walsh, M.; Roy, A.; Bianchetti, C.M.; Merchan, G. The potential of Thelypteris palustris and Asparagus sprengeri in phytoremediation of arsenic contamination. *Int. J. Phytoremediation* **2011**, *13*, 177–184. [CrossRef]
74. Hejna, M.; Moscatelli, A.; Stroppa, N.; Onelli, E.; Pilu, S.; Baldi, A.; Rossi, L. Bioaccumulation of heavy metals from wastewater through a Typha latifolia and Thelypteris palustris phytoremediation system. *Chemosphere* **2020**, *241*, 125018. [CrossRef]
75. Sciandrello, S.; Cambria, S.; Del Galdo, G.G.; Tavilla, G.; Minissale, P. Unexpected Discovery of Thelypteris palustris (Thelypteridaceae) in Sicily (Italy): Morphological, Ecological Analysis and Habitat Characterization. *Plants* **2021**, *10*, 2448. [CrossRef]
76. Mohammadzadeh, V.; Barani, M.; Amiri, M.S.; Taghavizadeh Yazdi, M.E.; Hassanisaadi, M.; Rahdar, A.; Varma, R.S. Applications of plant-based nanoparticles in nanomedicine: A review. *Sustain. Chem. Pharm.* **2022**, *25*, 100606. [CrossRef]
77. Sargazi, S.; Laraib, U.; Er, S.; Rahdar, A.; Hassanisaadi, M.; Zafar, M.N.; Díez-Pascual, A.M.; Bilal, M. Application of Green Gold Nanoparticles in Cancer Therapy and Diagnosis. *Nanomaterials* **2022**, *12*, 1102. [CrossRef]
78. Hashemi, S.F.; Tasharrofi, N.; Saber, M.M. Green synthesis of silver nanoparticles using Teucrium polium leaf extract and assessment of their antitumor effects against MNK45 human gastric cancer cell line. *J. Mol. Struct.* **2020**, *1208*, 127889. [CrossRef]
79. Pannerselvam, B.; Durai, P.; Thiyagarajan, D.; Song, H.J.; Kim, K.J.; Jung, Y.S.; Kim, H.J.; Rangarajulu, S.K. Facile Synthesis of Silver Nanoparticles Using Asian Spider Flower and Its In Vitro Cytotoxic Activity Against Human Breast Carcinoma Cells. *Processes* **2020**, *8*, 430. [CrossRef]
80. Hashim, N.; Paramasivam, M.; Tan, J.S.; Kernain, D.; Hussin, M.H.; Brosse, N.; Gambier, F.; Raja, P.B. Green mode synthesis of silver nanoparticles using Vitis vinifera's tannin and screening its antimicrobial activity/apoptotic potential versus cancer cells. *Mater. Today Commun.* **2020**, *25*, 101511. [CrossRef]
81. Cha, B.G.; Kim, J. Functional mesoporous silica nanoparticles for bio-imaging applications. *WIREs Nanomed. Nanobiotechnol.* **2019**, *11*, e1515. [CrossRef]
82. Zhang, K.; Zhao, Q.; Qin, S.; Fu, Y.; Liu, R.; Zhi, J.; Shan, C. Nanodiamonds conjugated upconversion nanoparticles for bio-imaging and drug delivery. *J. Colloid Interface Sci.* **2019**, *537*, 316–324. [CrossRef]
83. Kotcherlakota, R.; Nimushakavi, S.; Roy, A.; Yadavalli, H.C.; Mukherjee, S.; Haque, S.; Patra, C.R. Biosynthesized Gold Nanoparticles: In Vivo Study of Near-Infrared Fluorescence (NIR)-Based Bio-imaging and Cell Labeling Applications. *ACS Biomater. Sci. Eng.* **2019**, *5*, 5439–5452. [CrossRef]
84. Kwon, J.; Jun, S.W.; Kim, J.; Lee, M.; Choi, Y.; Kim, D.; Kim, M.; Lee, S.G.; Lee, S.; Kang, S.H.; et al. Excitation-dependent emissive FeSe nanoparticles induced by chiral interlayer expansion and their multi-color bio-imaging. *Nano Today* **2022**, *43*, 101424. [CrossRef]
85. Ansari, A.A.; Thakur, V.K.; Chen, G. Functionalized upconversion nanoparticles: New strategy towards FRET-based luminescence bio-sensing. *Coord. Chem. Rev.* **2021**, *436*, 213821. [CrossRef]
86. Varghese Alex, K.; Tamil Pavai, P.; Rugmini, R.; Shiva Prasad, M.; Kamakshi, K.; Sekhar, K.C. Green Synthesized Ag Nanoparticles for Bio-Sensing and Photocatalytic Applications. *ACS Omega* **2020**, *5*, 13123–13129. [CrossRef]
87. Agnihotri, A.S.; Varghese, A.; Nidhin, M. Transition metal oxides in electrochemical and bio sensing: A state-of-art review. *Appl. Surf. Sci. Adv.* **2021**, *4*, 100072. [CrossRef]

88. Mitchell, M.J.; Billingsley, M.M.; Haley, R.M.; Wechsler, M.E.; Peppas, N.A.; Langer, R. Engineering precision nanoparticles for drug delivery. *Nat. Rev. Drug Discov.* **2021**, *20*, 101–124. [CrossRef] [PubMed]
89. Manzano, M.; Vallet-Regí, M. Mesoporous Silica Nanoparticles for Drug Delivery. *Adv. Funct. Mater.* **2020**, *30*, 1902634. [CrossRef]
90. Sur, S.; Rathore, A.; Dave, V.; Reddy, K.R.; Chouhan, R.S.; Sadhu, V. Recent developments in functionalized polymer nanoparticles for efficient drug delivery system. *Nano-Struct. Nano-Obj.* **2019**, *20*, 100397. [CrossRef]
91. Delgado-Zegarra, J.; Alvarez-Risco, A.; Cárdenas, C.; Donoso, M.; Moscoso, S.; Rojas Román, B.; Del-Aguila-Arcentales, S.; Davies, N.M.; Yáñez, J.A. Labeling of Genetically Modified (GM) Foods in Peru: Current Dogma and Insights of the Regulatory and Legal Statutes. *Int. J. Food Sci.* **2022**, *2022*, 3489785. [CrossRef] [PubMed]
92. Delgado-Zegarra, J.; Alvarez-Risco, A.; Yáñez, J.A. Uso indiscriminado de pesticidas y ausencia de control sanitario para el mercado interno en Perú. *Rev. Panam. Salud. Publica* **2018**, *42*, e3. [CrossRef]
93. Mejia-Meza, E.I.; Yáñez, J.A.; Davies, N.M.; Clary, C.D. Dried Raspberries: Phytochemicals and Health Effects. In *Dried Fruits*; John Wiley & Sons, Inc.: Hoboken, NJ, USA, 2013; pp. 161–174.
94. Mejia-Meza, E.I.; Yanez, J.A.; Davies, N.M.; Rasco, B.; Younce, F.; Remsberg, C.M.; Clary, C. Improving nutritional value of dried blueberries (*Vaccinium corymbosum* L.) combining microwave-vacuum, hot-air drying and freeze-drying technologies. *Int. J. Food Eng.* **2008**, *4*, 1–6. [CrossRef]
95. Mejia-Meza, E.I.; Yanez, J.A.; Remsberg, C.M.; Takemoto, J.K.; Davies, N.M.; Rasco, B.; Clary, C. Effect of dehydration on raspberries: Polyphenol and anthocyanin retention, antioxidant capacity, and antiadipogenic activity. *J. Food Sci.* **2010**, *75*, H5–H12. [CrossRef]
96. Ramos-Escudero, D.F.; Condezo-Hoyos, L.A.; Ramos-Escudero, M.; Yanez, J.A. Design and assessment of the in vitro anti-oxidant capacity of a beverage composed of green tea (*Camellia sinensis* L.) and lemongrass (*Cymbopogon citratus* Stap). In *Handbook of Green Tea and Health Research*; McKinley, H., Jamieson, M., Eds.; Nova Science Publishers, Inc.: New York, NY, USA, 2009; pp. 81–101.
97. Ramos-Escudero, D.F.; Munoz, A.M.; Alvarado-Ortiz, C.; Yanez, J.A. Antocianinas, polifenoles, actividad anti-oxidante de sachapapa morada (*Dioscorea trifida* L.) y evaluación de lipoperoxidación en suero humano. *Rev. Soc. Quím. Perú* **2010**, *76*, 61–72.
98. Ramos-Escudero, F.; Muñoz, A.M.; Alvarado-Ortíz, C.; Alvarado, Á.; Yáñez, J.A. Purple corn (*Zea mays* L.) phenolic compounds profile and its assessment as an agent against oxidative stress in isolated mouse organs. *J. Med. Food* **2012**, *15*, 206–215. [CrossRef]
99. Ramos-Escudero, M.; Ramos-Escudero, D.F.; Remsberg, C.M.; Takemoto, J.K.; Davies, N.M.; Yanez, J.A. Identification of Polyphenols and Anti-Oxidant Capacity of *Piper aduncum* L. *Open Bioact. Compd. J.* **2008**, *1*, 18–21. [CrossRef]
100. Forrest, M.L.; Yanez, J.A.; Remsberg, C.M.; Ohgami, Y.; Kwon, G.S.; Davies, N.M. Paclitaxel prodrugs with sustained release and high solubility in poly(ethylene glycol)-b-poly(epsilon-caprolactone) micelle nanocarriers: Pharmacokinetic disposition, tolerability, and cytotoxicity. *Pharm. Res.* **2008**, *25*, 194–206. [CrossRef] [PubMed]
101. Roupe, K.; Remsberg, C.; Yanez, J.; Davies, N. Pharmacometrics of Stilbenes: Seguing Towards the Clinic. *Curr. Clin. Pharmacol.* **2006**, *1*, 81–101. [CrossRef] [PubMed]
102. Louizos, C.; Yáñez, J.A.; Forrest, M.L.; Davies, N.M. Understanding the hysteresis loop conundrum in pharmacokinetic/pharmacodynamic relationships. *J. Pharm. Pharm. Sci.* **2014**, *17*, 34–91. [CrossRef]
103. Yáñez, J.A.; Remsberg, C.M.; Sayre, C.L.; Forrest, M.L.; Davies, N.M. Flip-flop pharmacokinetics–delivering a reversal of disposition: Challenges and opportunities during drug development. *Ther. Deliv.* **2011**, *2*, 643–672. [CrossRef]
104. Davies, N.M.; Takemoto, J.K.; Brocks, D.R.; Yáñez, J.A. Multiple peaking phenomena in pharmacokinetic disposition. *Clin. Pharmacokinet.* **2010**, *49*, 351–377. [CrossRef] [PubMed]
105. Yáñez, J.A.; Andrews, P.K.; Davies, N.M. Methods of analysis and separation of chiral flavonoids. *J. Chromatogr. B Anal. Technol. Biomed. Life Sci.* **2007**, *848*, 159–181. [CrossRef] [PubMed]
106. Vega-Villa, K.R.; Yanez, J.A.; Remsberg, C.M.; Ohgami, Y.; Davies, N.M. Stereospecific high-performance liquid chromatographic validation of homoeriodictyol in serum and Yerba Santa (*Eriodictyon glutinosum*). *J. Pharm. Biomed. Anal.* **2007**, *46*, 971–974. [CrossRef] [PubMed]
107. Takemoto, J.K.; Remsberg, C.M.; Yanez, J.A.; Vega-Villa, K.R.; Davies, N.M. Stereospecific analysis of sakuranetin by high-performance liquid chromatography: Pharmacokinetic and botanical applications. *J. Chromatogr. B Analyt. Technol. Biomed. Life Sci.* **2008**, *875*, 136–141. [CrossRef]
108. Yáñez, J.A.; Chemuturi, N.V.; Womble, S.W.; Sayre, C.L.; Davies, N.M. Flavonoids and Drug Interactions. In *Flavonoid Pharmacokinetics: Methods of Analysis, Preclinical and Clinical Pharmacokinetics, Safety, and Toxicology*; Davies, N.M., Yáñez, J.A., Eds.; John Wiley & Sons: Hoboken, NJ, USA, 2012; pp. 281–319.
109. Davies, N.M.; Yáñez, J.A. *Flavonoid Pharmacokinetics: Methods of Analysis, Preclinical and Clinical Pharmacokinetics, Safety, and Toxicology*; Davies, N.M., Yáñez, J.A., Eds.; John Wiley & Sons: Hoboken, NJ, USA, 2012; p. 352.
110. Vega-Villa, K.R.; Remsberg, C.M.; Podelnyk, K.L.; Davies, N.M. Stereospecific high-performance liquid chromatographic assay of isosakuranetin in rat urine. *J. Chromatogr. B Analyt. Technol. Biomed. Life Sci.* **2008**, *875*, 142–147. [CrossRef]
111. Serve, K.M.; Yáñez, J.A.; Remsberg, C.M.; Davies, N.M.; Black, M.E. Development and validation of a rapid and sensitive HPLC method for the quantification of 5-fluorocytosine and its metabolites. *Biomed. Chromatogr.* **2010**, *24*, 556–561. [CrossRef]
112. Yáñez, J.A.; Sayre, C.L.; Martinez, S.E.; Davies, N.M. Chiral Methods of Flavonoid Analysis. In *Flavonoid Pharmacokinetics: Methods of Analysis, Preclinical and Clinical Pharmacokinetics, Safety, and Toxicology*; Davies, N.M., Yáñez, J.A., Eds.; John Wiley & Sons: Hoboken, NJ, USA, 2012; pp. 117–159.

113. Yáñez, J.A.; Sayre, C.L.; Davies, N.M. Preclinical Pharmacokinetics of Flavonoids. In *Flavonoid Pharmacokinetics: Methods of Analysis, Preclinical and Clinical Pharmacokinetics, Safety, and Toxicology*; Davies, N.M., Yáñez, J.A., Eds.; John Wiley & Sons: Hoboken, NJ, USA, 2012; pp. 161–193.
114. Sayre, C.L.; Gerde, K.D.; Yáñez, J.A.; Davies, N.M. Clinical Pharmacokinetics of Flavonoids. In *Flavonoid Pharmacokinetics: Methods of Analysis, Preclinical and Clinical Pharmacokinetics, Safety, and Toxicology*; Davies, N.M., Yáñez, J.A., Eds.; John Wiley & Sons: Hoboken, NJ, USA, 2012; pp. 195–247.
115. Yanez, J.A.; Brocks, D.R.; Forrest, M.L.; Davies, N.M. Pharmacokinetic Behaviors of Orally Administered Drugs. In *Oral Bioavailability: Basic Principles, Advanced Concepts, and Applications*; Hu, M., Li, X., Eds.; John Wiley & Sons, Inc.: Hoboken, NJ, USA, 2011; pp. 183–220.
116. Davies, N.M.; Yáñez, J.A. Front Matter. In *Flavonoid Pharmacokinetics: Methods of Analysis, Preclinical and Clinical Pharmacokinetics, Safety, and Toxicology*; Davies, N.M., Yáñez, J.A., Eds.; John Wiley & Sons: Hoboken, NJ, USA, 2012; pp. i–xv.
117. Yanez, J.A.; Wang, S.W.; Knemeyer, I.W.; Wirth, M.A.; Alton, K.B. Intestinal lymphatic transport for drug delivery. *Adv. Drug Deliv. Rev.* **2011**, *63*, 923–942. [CrossRef] [PubMed]
118. Chemuturi, N.; Yanez, J.A. The role of xenobiotic transporters in ophthalmic drug delivery. *J. Pharm. Pharm. Sci.* **2013**, *16*, 683–707. [CrossRef] [PubMed]
119. Vega-Villa, K.R.; Takemoto, J.K.; Yanez, J.A.; Remsberg, C.M.; Forrest, M.L.; Davies, N.M. Clinical toxicities of nanocarrier systems. *Adv. Drug Deliv. Rev.* **2008**, *60*, 929–938. [CrossRef] [PubMed]
120. Yanez, J.A.; Teng, X.W.; Roupe, K.A.; Davies, N.M. Alternative Methods for Assessing Experimental Colitis In Vivo and Ex Vivo. *J. Med. Sci.* **2006**, *6*, 356–365. [CrossRef]
121. Chung, S.A.; Olivera, S.; Rojas Román, B.; Alanoca, E.; Moscoso, S.; Limpias Terceros, B.; Alvarez-Risco, A.; Yáñez, J.A. Temáticas de la producción científica de la Revista Cubana de Farmacia indizada en Scopus (1967–2020). *Rev. Cuba. De Farm.* **2021**, *54*, 1–46.
122. Singh, T.A.; Das, J.; Sil, P.C. Zinc oxide nanoparticles: A comprehensive review on its synthesis, anticancer and drug delivery applications as well as health risks. *Adv. Colloid Interface Sci.* **2020**, *286*, 102317. [CrossRef]
123. Khodashenas, B.; Ghorbani, H.R. Synthesis of copper nanoparticles: An overview of the various methods. *Korean J. Chem. Eng.* **2014**, *31*, 1105–1109. [CrossRef]
124. He, W.; Tian, H.; Zhang, S.; Ying, H.; Meng, Z.; Han, W. Scalable synthesis of Si/C anode enhanced by FeSix nanoparticles from low-cost ferrosilicon for lithium-ion batteries. *J. Power Sources* **2017**, *353*, 270–276. [CrossRef]
125. Rane, A.V.; Kanny, K.; Abitha, V.K.; Thomas, S. Chapter 5—Methods for Synthesis of Nanoparticles and Fabrication of Nanocomposites. In *Synthesis of Inorganic Nanomaterials*; Mohan Bhagyaraj, S., Oluwafemi, O.S., Kalarikkal, N., Thomas, S., Eds.; Woodhead Publishing: Shaston, UK, 2018; pp. 121–139.
126. Jadoun, S.; Arif, R.; Jangid, N.K.; Meena, R.K. Green synthesis of nanoparticles using plant extracts: A review. *Environ. Chem. Lett.* **2021**, *19*, 355–374. [CrossRef]
127. Salem, S.S.; Fouda, A. Green Synthesis of Metallic Nanoparticles and Their Prospective Biotechnological Applications: An Overview. *Biol. Trace Elem. Res.* **2021**, *199*, 344–370. [CrossRef]
128. Naikoo, G.A.; Mustaqeem, M.; Hassan, I.U.; Awan, T.; Arshad, F.; Salim, H.; Qurashi, A. Bioinspired and green synthesis of nanoparticles from plant extracts with antiviral and antimicrobial properties: A critical review. *J. Saudi Chem. Soc.* **2021**, *25*, 101304. [CrossRef]
129. Jacob, J.M.; Ravindran, R.; Narayanan, M.; Samuel, S.M.; Pugazhendhi, A.; Kumar, G. Microalgae: A prospective low cost green alternative for nanoparticle synthesis. *Curr. Opin. Environ. Sci. Health* **2021**, *20*, 100163. [CrossRef]
130. Zea Álvarez, J.L.; Talavera Núñez, M.E.; Arenas Chávez, C.; Pacheco Salazar, D.; Osorio Anaya, A.M.; Vera Gonzales, C. Obtención y caracterización del nanocomposito: Nanopartículas de plata y carboximetilquitosano (NPsAg-CMQ). *Rev. De La Soc. Química Del Perú* **2019**, *85*, 14–24. [CrossRef]
131. Quispe-Quispe, L.G.; Limpe-Ramos, P.; Arenas Chávez, C.A.; Gomez, M.M.; Mejia, C.R.; Alvarez-Risco, A.; Del-Aguila-Arcentales, S.; Yáñez, J.A.; Vera-Gonzales, C. Physical and mechanical characterization of a functionalized cotton fabric with nanocomposite based on silver nanoparticles and carboxymethyl chitosan using green chemistry. *Processes* **2022**, *10*, 1207. [CrossRef]
132. Arenas-Chávez, C.A.; Hollanda, L.M.; Arce-Esquivel, A.A.; Alvarez-Risco, A.; Del-Aguila-Arcentales, S.; Yáñez, J.A.; Vera-Gonzales, C. Antibacterial and Antifungal Activity of Functionalized Cotton Fabric with Nanocomposite Based on Silver Nanoparticles and Carboxymethyl Chitosan. *Processes* **2022**, *10*, 1088. [CrossRef]
133. Baskaran, X.-R.; Geo Vigila, A.-V.; Zhang, S.-Z.; Feng, S.-X.; Liao, W.-B. A review of the use of pteridophytes for treating human ailments. *J. Zhejiang Univ. Sci. B* **2018**, *19*, 85–119. [CrossRef]
134. Mehwish, H.M.; Rajoka, M.S.R.; Xiong, Y.; Cai, H.; Aadil, R.M.; Mahmood, Q.; He, Z.; Zhu, Q. Green synthesis of a silver nanoparticle using Moringa oleifera seed and its applications for antimicrobial and sun-light mediated photocatalytic water detoxification. *J. Environ. Chem. Eng.* **2021**, *9*, 105290. [CrossRef]
135. Huq, M.A. Green Synthesis of Silver Nanoparticles Using Pseudoduganella eburnea MAHUQ-39 and Their Antimicrobial Mechanisms Investigation against Drug Resistant Human Pathogens. *Int. J. Mol. Sci.* **2020**, *21*, 1510. [CrossRef]
136. Alsammarraie, F.K.; Wang, W.; Zhou, P.; Mustapha, A.; Lin, M. Green synthesis of silver nanoparticles using turmeric extracts and investigation of their antibacterial activities. *Colloids Surf. B Biointerfaces* **2018**, *171*, 398–405. [CrossRef]

137. Gangapuram, B.R.; Bandi, R.; Alle, M.; Dadigala, R.; Kotu, G.M.; Guttena, V. Microwave assisted rapid green synthesis of gold nanoparticles using Annona squamosa L peel extract for the efficient catalytic reduction of organic pollutants. *J. Mol. Struct.* **2018**, *1167*, 305–315. [CrossRef]
138. Ismail, M.; Gul, S.; Khan, M.I.; Khan, M.A.; Asiri, A.M.; Khan, S.B. Green synthesis of zerovalent copper nanoparticles for efficient reduction of toxic azo dyes congo red and methyl orange. *Green Processing Synth.* **2019**, *8*, 135–143. [CrossRef]
139. Ijaz, I.; Gilani, E.; Nazir, A.; Bukhari, A. Detail review on chemical, physical and green synthesis, classification, characterizations and applications of nanoparticles. *Green Chem. Lett. Rev.* **2020**, *13*, 223–245. [CrossRef]
140. Choudhary, M.K.; Kataria, J.; Sharma, S. Evaluation of the kinetic and catalytic properties of biogenically synthesized silver nanoparticles. *J. Clean. Prod.* **2018**, *198*, 882–890. [CrossRef]
141. Dehghanizade, S.; Arasteh, J.; Mirzaie, A. Green synthesis of silver nanoparticles using Anthemis atropatana extract: Characterization and in vitro biological activities. *Artif. Cells Nanomed. Biotechnol.* **2018**, *46*, 160–168. [CrossRef] [PubMed]
142. Govender, R.; Phulukdaree, A.; Gengan, R.M.; Anand, K.; Chuturgoon, A.A. Silver nanoparticles of Albizia adianthifolia: The induction of apoptosis in human lung carcinoma cell line. *J. Nanobiotechnol.* **2013**, *11*, 5. [CrossRef]
143. Gengan, R.M.; Anand, K.; Phulukdaree, A.; Chuturgoon, A. A549 lung cell line activity of biosynthesized silver nanoparticles using Albizia adianthifolia leaf. *Colloids Surf. B Biointerfaces* **2013**, *105*, 87–91. [CrossRef]
144. Maroyi, A. Albizia Adianthifolia: Botany, Medicinal Uses, Phytochemistry, and Pharmacological Properties. *Sci. World J.* **2018**, *2018*, 7463584. [CrossRef]
145. Liu, B.; Li, X.; Zheng, C.; Wang, X.; Sun, R. Facile and green synthesis of silver nanoparticles in quaternized carboxymethyl chitosan solution. *Nanotechnology* **2013**, *24*, 235601. [CrossRef]
146. Tripathi, D.; Modi, A.; Narayan, G.; Rai, S.P. Green and cost effective synthesis of silver nanoparticles from endangered medicinal plant Withania coagulans and their potential biomedical properties. *Mater. Sci. Eng. C* **2019**, *100*, 152–164. [CrossRef]
147. Jiang, S.; Hua, L.; Guo, Z.; Sun, L. One-pot green synthesis of doxorubicin loaded-silica nanoparticles for in vivo cancer therapy. *Mater. Sci. Eng. C* **2018**, *90*, 257–263. [CrossRef]
148. Zhang, X.-F.; Liu, Z.-G.; Shen, W.; Gurunathan, S. Silver Nanoparticles: Synthesis, Characterization, Properties, Applications, and Therapeutic Approaches. *Int. J. Mol. Sci.* **2016**, *17*, 1534. [CrossRef] [PubMed]
149. Kumara Swamy, M.; Sudipta, K.M.; Jayanta, K.; Balasubramanya, S. The green synthesis, characterization, and evaluation of the biological activities of silver nanoparticles synthesized from Leptadenia reticulata leaf extract. *Appl. Nanosci.* **2015**, *5*, 73–81. [CrossRef]
150. Daphedar, A.; Taranath, T.C. Biosynthesis of silver nanoparticles by leaf extract of Albizia saman (Jacq.) Merr. and their cytotoxic effect on mitotic chromosomes of Drimia indica (Roxb.) Jessop. *Environ. Sci. Pollut. Res.* **2017**, *24*, 25861–25869. [CrossRef] [PubMed]
151. Premasudha, P.; Venkataramana, M.; Abirami, M.; Vanathi, P.; Krishna, K.; Rajendran, R. Biological synthesis and characterization of silver nanoparticles using Eclipta alba leaf extract and evaluation of its cytotoxic and antimicrobial potential. *Bull. Mater. Sci.* **2015**, *38*, 965–973. [CrossRef]
152. Arya, G.; Kumari, R.M.; Gupta, N.; Kumar, A.; Chandra, R.; Nimesh, S. Green synthesis of silver nanoparticles using Prosopis juliflora bark extract: Reaction optimization, antimicrobial and catalytic activities. *Artif. Cells Nanomed. Biotechnol.* **2018**, *46*, 985–993. [CrossRef]
153. Souza, T.G.F.; Ciminelli, V.S.T.; Mohallem, N.D.S. A comparison of TEM and DLS methods to characterize size distribution of ceramic nanoparticles. *J. Phys. Conf. Ser.* **2016**, *733*, 012039. [CrossRef]
154. Caputo, F.; Clogston, J.; Calzolai, L.; Rösslein, M.; Prina-Mello, A. Measuring particle size distribution of nanoparticle enabled medicinal products, the joint view of EUNCL and NCI-NCL. A step by step approach combining orthogonal measurements with increasing complexity. *J. Control. Release* **2019**, *299*, 31–43. [CrossRef]
155. Mahl, D.; Diendorf, J.; Meyer-Zaika, W.; Epple, M. Possibilities and limitations of different analytical methods for the size determination of a bimodal dispersion of metallic nanoparticles. *Colloids Surf. A Physicochem. Eng. Asp.* **2011**, *377*, 386–392. [CrossRef]
156. *ISO 22412:2017*; Particle Size Analysis—Dynamic Light Scattering (DLS). ISO: Geneva, Switzerland, 2017.
157. Remya, R.R.; Rajasree, S.R.R.; Aranganathan, L.; Suman, T.Y. An investigation on cytotoxic effect of bioactive AgNPs synthesized using Cassia fistula flower extract on breast cancer cell MCF-7. *Biotechnol. Rep.* **2015**, *8*, 110–115. [CrossRef]
158. Singh, P.; Kim, Y.J.; Singh, H.; Wang, C.; Hwang, K.H.; Farh, M.E.-A.; Yang, D.C. Biosynthesis, characterization, and antimicrobial applications of silver nanoparticles. *Int. J. Nanomed.* **2015**, *10*, 2567–2577. [CrossRef]
159. Jha, D.; Thiruveedula, P.K.; Pathak, R.; Kumar, B.; Gautam, H.K.; Agnihotri, S.; Sharma, A.K.; Kumar, P. Multifunctional biosynthesized silver nanoparticles exhibiting excellent antimicrobial potential against multi-drug resistant microbes along with remarkable anticancerous properties. *Mater. Sci. Eng. C* **2017**, *80*, 659–669. [CrossRef] [PubMed]
160. Prabhu, D.; Arulvasu, C.; Babu, G.; Manikandan, R.; Srinivasan, P. Biologically synthesized green silver nanoparticles from leaf extract of *Vitex negundo* L. induce growth-inhibitory effect on human colon cancer cell line HCT15. *Process Biochem.* **2013**, *48*, 317–324. [CrossRef]
161. Beyene, H.D.; Werkneh, A.A.; Bezabh, H.K.; Ambaye, T.G. Synthesis paradigm and applications of silver nanoparticles (AgNPs), a review. *Sustain. Mater. Technol.* **2017**, *13*, 18–23. [CrossRef]

162. Ratan, Z.A.; Haidere, M.F.; Nurunnabi, M.; Shahriar, S.M.; Ahammad, A.J.S.; Shim, Y.Y.; Reaney, M.J.T.; Cho, J.Y. Green Chemistry Synthesis of Silver Nanoparticles and Their Potential Anticancer Effects. *Cancers* **2020**, *12*, 855. [CrossRef]
163. Ahmad, S.; Munir, S.; Zeb, N.; Ullah, A.; Khan, B.; Ali, J.; Bilal, M.; Omer, M.; Alamzeb, M.; Salman, S.M.; et al. Green nanotechnology: A review on green synthesis of silver nanoparticles—an ecofriendly approach. *Int. J. Nanomed.* **2019**, *14*, 5087–5107. [CrossRef]
164. Jeyaraj, M.; Rajesh, M.; Arun, R.; MubarakAli, D.; Sathishkumar, G.; Sivanandhan, G.; Dev, G.K.; Manickavasagam, M.; Premkumar, K.; Thajuddin, N.; et al. An investigation on the cytotoxicity and caspase-mediated apoptotic effect of biologically synthesized silver nanoparticles using Podophyllum hexandrum on human cervical carcinoma cells. *Colloids Surf. B Biointerfaces* **2013**, *102*, 708–717. [CrossRef]
165. Bonjar, L.S. "Nanogold detoxifying machine" to remove idle nanogold particles from blood stream of cancer patients treated with antibody-nanogold therapeutics. *Med. Hypotheses* **2013**, *80*, 601–605. [CrossRef]